# Resistance of a one-dimensional quasicrystal: Power-law growth

Bill Sutherland and Mahito Kohmoto
*Department of Physics, University of Utah, Salt Lake City, Utah 84112*
(Received 6 March 1987)

Properties of the electrical resistance of a one-dimensional quasicrystal, whose structure is governed by the Fibonacci rule, are studied by means of the Landauer formula. In particular, it is shown that the growth of the resistance with sample length is bounded by a power law for certain energies. More specifically, the resistance is shown to grow with sample length not as a single power, but with a spectrum of exponents. These exact results are illustrated by examples. It is conjectured that such behavior is typical for the entire spectrum.

## I. INTRODUCTION

A quasiperiodic Schrödinger equation using the Fibonacci sequence was introduced by Kohmoto, Kadanoff, and Tang[1] and given independently by Ostlund *et al.*[2] in 1983. The most striking feature of the model is that the spectrum is purely singularly continuous—namely, all the states are critical.[3] (Remember that all states are localized for disordered systems in one dimension, while other quasiperiodic systems can have states of all three types—localized, extended, or critical—depending on the values of the coupling constant and energy.[4])

If the Fermi energy is in the region of localized states of the spectrum (dense point spectrum), it is known that the electrical resistance grows exponentially with the sample size, and the rate of exponential growth gives the localization length of the state at the Fermi energy. For the critical states, on the other hand, the localization length is not defined—or is effectively infinite—and it is thus of interest to study the behavior of the electrical resistance as the sample size is increased.

It is most common to express the resistance of a one-dimensional system in terms of the transmission and reflection coefficients by means of the Landauer formula.[5] In the present case of a quasiperiodic system, however, the use of the Landauer formula must be examined carefully. Since the spectrum is a Cantor set with zero Lebesgue measure—namely, the energy gaps are dense everywhere in the spectrum—it is likely that the linear response to a weak electric field cannot be defined properly.

Nonetheless, we adopt the Landauer formula as a working definition of resistance. Therefore this resistance must be thought of as a parameter which characterizes the states, rather than the coefficient of a linear response.

The outline of the paper is as follows. In Sec. II we review the transfer-matrix method for the multiscatterer problem, and give the Landauer formula for the resistance in terms of this transfer matrix. Section III defines the particular one-dimensional quasiperiodic system we will investigate, built according to the Fibonacci scheme, with two types of scatterers in the ratio of the golden mean. Also, this part reviews the very important trace map. Section IV discusses in some depth the structure of the transfer matrices. First, the consequences for the transfer matrices of the structure in the trace map are explicitly spelled out. Second, we give a proof that the growth of the resistance with sample length is bounded by a power law, at a fixed point of the trace map. Finally, we argue for a more general conjecture. In Sec. V we present examples, numerical experiments, and pictures to illustrate the general results of the previous part. Section VI is a short summary.

## II. THE TRANSFER-MATRIX METHOD AND THE LANDAUER FORMULA

In this part of the paper the formalism for calculating the resistance of a one-dimensional sample from the transfer matrix through the Landauer formula is introduced. This is used in the rest of the paper for our investigation of the quasiperiodic system. For a detailed derivation of this formalism and more extensive discussions see Kohmoto.[6]

Let us consider a one-dimensional system with $n$ scatters. The transfer matrix $T(n)$ for the total system is the product of the transfer matrices $M(j)$ for the individual sites $j$, so that

$$T(n)=M(n)M(n-1)\cdots M(j)\cdots M(2)M(1)\ .$$

The transfer matrix $M(n)$ corresponding to the $n$th scatter is of the form

$$M(n)=U(n)[V(n)]^{-1}$$

with

$$U(n)=\begin{bmatrix} \mathrm{Re}\,t(n) & 1+\mathrm{Re}\,r(n) \\ -\mathrm{Im}\,t(n) & -\mathrm{Im}\,r(n) \end{bmatrix},$$

$$V(n)=\begin{bmatrix} 1+\mathrm{Re}\,r(n) & \mathrm{Re}\,t(n) \\ \mathrm{Im}\,r(n) & \mathrm{Im}\,t(n) \end{bmatrix}.$$

Here $t(n)$ and $r(n)$ are the transmission and reflection coefficients for the $n$th scatterer, and Re and Im signify the real and imaginary parts, respectively.

Since each transfer matrix $M(n)$ is a real $2\times 2$ matrix with determinant 1, then the total transfer matrix $T(n)$ of the system is also a real $2\times 2$ matrix with determinant 1. Note that the transfer matrices will depend upon the energy through the transmission and reflection coefficients.

According to the Landauer formula,[5] the resistance $\rho$ of the system is given by

$$\rho = |r(\text{total})|^2/|t(\text{total})|^2 ,$$

where r(total) and t(total) are the reflection and transmission coefficients of the total system.

This formula is compactly written in terms of the transfer matrix as

$$\rho(n) = \{\mathrm{Tr}[{}^tT(n)T(n)]/2-1\}/2 .$$

Here Tr denotes the trace of the matrix, ${}^tT$ is the transpose of $T$, and the particular combination $\mathrm{Tr}[{}^tT(n)T(n)]$—equal to the sum of the squares of the four matrix elements of $T(n)$— will play a crucial role in Sec. IV.

## III. THE FIBONACCI CRYSTAL AND THE TRACE MAP

Henceforth, we exclusively consider a system in which the scatterers are arranged following the Fibonacci sequence. Consider only two types of scatterers, called $A$ and $B$. Then the Fibonacci sequence is defined recursively by

$$S_{k+1} = S_{k-1} + S_k ,$$

with

$$S_1 = \{A\},\quad S_0 = \{B\} .$$

Addition is here understood as simply the joining of sequences or concatenation of symbols. $S_k$ is an element of the free group generated by the elements $A,B$, with no further defining relations; we can read from it the entire sequence of $F_k$ elements. ($F_k$— the number of elements in the sequence $S_k$—is a Fibonacci number, defined similarly as $F_{k+1}=F_{k-1}+F_k$, for $k\geq 1$ with $F_0=1$ and $F_1=1$.) Asymptotically, $F_k\to\phi^k$, as $k\to\infty$, where $\phi$ is the golden mean, equal to $(1+\sqrt{5})/2$.

We shall denote the transfer matrices corresponding to the scatters $A$ and $B$ by the same symbols— $A$ and $B$. This will cause no confusion. Then $M(n)$ is either $A$ or $B$. Therefore, a total transfer matrix $T(F_k)$ for the Fibonacci sequence $S_k$, is a product of $F_k$ matrices, each of which is either $A$ or $B$.

Let us denote the Fibonacci transfer matrices $T(F_k)$ by $T_k$ for simplicity. Then one has the recursion relation for the transfer matrices[1,2]

$$T_{k+1} = T_{k-1}T_k ,$$

with $T_0=B$ and $T_1=A$. This equation can be thought of as a six-dimensional map, since each of the matrices $T_k$ are specified by three real parameters. We call this recursion relation the Fibonacci dynamics, for reasons that will be made clear.

In fact, there is a three-dimensional submap[1] of the above matrix map, which maps the traces of three successive Fibonacci matrices. Thus, writing $x_k=\mathrm{Tr}(T_k)/2$, we find the trace map to be

$$x_{k+1} = 2x_kx_{k-1} - x_{k-2} .$$

This map has a constant of motion (invariant) given by

$$\mathcal{J} = x_{k+1}^2 + x_k^2 + x_{k-1}^2 - 2x_{k+1}x_kx_{k-1} - 1 .$$

The constant of motion is always positive and gives a measure of the difference of the strength of the scattering from the two types of $A$ and $B$ scatterers; when $A=B$, then $\mathcal{J}=0$.

The spectrum of the infinite system $S_\infty$, which is truly quasiperiodic, is the set of all energies which give a bounded orbit $\{x_k\}$ of the trace map.[1,7,8] Note that the matrices $A$ and $B$, and hence the initial point of the trace map, depend upon the energy through the reflection and transmission coefficients. Also, the constant of motion depends upon the energy. This is a different situation from the tight-binding models of quasicrystals, where the constant of motion is independent of energy.[9]

We are interested in the behavior of the resistance when the energy is in the spectrum, or equivalently when the trace of $M_k$ is bounded. Almost all of the orbits $\{x_k\}$ of the trace map are unbounded, escaping to infinity exponentially fast in $k$, and this implies that the Lebesque measure of the spectrum is zero. The bounded orbits exist with zero measure with respect to the energy. There are two types of bounded orbits: periodic and chaotic. The periodic orbits are fixed points of the $Q$-times iterated trace map or $Q$-cycles for short. We largely focus our subsequent analysis of the resistance of the periodic orbits, since the chaotic orbits are difficult to treat. We deduce some properties of the chaotic orbits from a knowledge of the periodic orbits.

## IV. STRUCTURE OF THE TRANSFER MATRICES

This section is a rather difficult part of the paper, since it requires close reasoning, yet it is crucial to the entire argument of this paper. We therefore have placed the mathematical details in a long appendix, and here draw on the two principal results which we will need to discuss the power-law growth of the resistance as a function of sample size. In Sec. V we provide examples and illustrations.

The first result we need is an answer to the question: When we have a $Q$-cycle of the trace map, so that $x_{k+Q}=x_k$, how are the transfer matrices $T_{k+Q}$ and $T_k$ related? The result[10] we find in the Appendix is that there exists a matrix $L$—a real, $2\times 2$ matrix with determinant 1, independent of $k$—such that

$$T_{j+Q} = LT_jL^{-1} .$$

Thus translation of the index $j$ by $Q$, is given by a similarity transformation of the transfer matrices.

The second result we need concerns the size $|T|$ of a transfer matrix $T$, defined by

$$|T|^2 = \mathrm{Tr}({}^tTT)/2 .$$

(The symbol ${}^tT$ denotes the transpose of $T$.) Then in the Appendix we show that for two transfer matrices $A$ and $C$,

$$|AC|^2 \le 2|A|^2|C|^2 .$$

This gives as a simple corollary that

$$|CAC^{-1}| \le 2|A|\ |C|^2 .$$

With these two results, we now proceed to estimate the growth of the transfer matrices $T(n)$. In general, we can expect these matrices to grow exponentially in the lattice index $n$. However, if we have a $Q$-cycle, this is not the case, as we shall see, and instead we will have a power-law growth at most.

As we found in the Appendix, and quoted above, for a $Q$-cycle

$$T_{j+Q}=LT_jL^{-1} .$$

Combining this result with the previous corollary, derived in the Appendix, we estimate the growth of the transfer matrices on the Fibonacci points as

$$|T_{j+kQ}| \le (2|L|^2)^k|T_j| .$$

This, however, is not what we want. Instead, we wish to bound the growth of $|T(n)|$ with increasing $n$.

We introduce the symbol $|\underline{T}_j|$ to denote the maximum value of $|T(n)|$ for $n$ from 1 to $F_j$. Then by definition, $|\underline{T}_j| \le |\underline{T}_{j+k}|$, and $|T(n)| \le |\underline{T}_j|$ for $n \le F_j$.

For the free group—just the sequences of $A$'s and $B$'s—we found that we could inflate a sequence $S_k$ to a sequence $S_{k+Q}$ by the substitution $[B,A] \to [S_Q, S_{1+Q}]$. Thus, we find that $T(n)$, with $n \le F_j$, inflates to

$$T(n) \to T'(n)=T(n')=LT(n)L^{-1} ,$$

with $n' \le F_{j+Q}$. Therefore,

$$|T'(n)|=|T(n')| \le 2|L|^2|T(n)| .$$

Writing $T(n+1)=M(n+1)T(n)$, after inflation we find that this inflates to

$$T(n'+m)=T(m)T(n') ,$$

with $n+m \le (n+1)'$ or $m \le F_{Q+1}$.

Applying the inequality once again,

$$\begin{aligned}|T(n'+m)| &\le \sqrt{2}|T(m)|\ |T(n')| \\ &\le 2\sqrt{2}|L|^2|T(m)|\ |T(n)| .\end{aligned}$$

Now allowing $n$ to range from 1 to $F_j$ and $m$ to range from 1 to $F_{Q+1}$, then $n'+m$ will range from 1 to $F_{j+Q}$. Thus, we have the final inequality, for a $Q$-cycle, that

$$|\underline{T}_{j+Q}| \le 2\sqrt{2}|L|^2|\underline{T}_{Q+1}|\ |\underline{T}_j| .$$

We may apply this inequality repeatedly. Let the scale factor be

$$t=2\sqrt{2}|L|^2|\underline{T}_{Q+1}| .$$

Then we find that

$$|\underline{T}_{j+kQ}| \le t^k|\underline{T}_j| .$$

Combining these results with the previous expression for the resistivity,

$$\rho(n)=[|T(n)|^2-1]/2 ,$$

we find the asymptotic bound for the resistivity at a $Q$-cycle as

$$\rho(n) \le \rho_0 n^{\alpha} ,$$

with

$$\alpha=\ln(t)/\ln(\phi^Q) ,$$

where $\phi$ is the golden mean, equal to $(1+\sqrt{5})/2$.

Suppose now we were to consider the other states in the spectrum, corresponding to the chaotic orbits instead of the periodic $Q$-cycles of the trace map. These orbits lie on the two-dimensional surface defined by the constant of the motion $\mathcal{J}$ fixed, and are bounded. One can define an area on this invariant surface which is preserved by the trace map. We make the following conjecture.

*Conjecture I.* For all points in the spectrum, the resistance as a function of sample size is bounded by a power of the sample length.

On the other hand, suppose we found a point where the resistance was bounded by a power of the sample length: would this point be in the spectrum? By the inequality shown in the Appendix, the trace is also bounded by a power, since it can grow no faster than the square of the resistance. Suppose the orbit of the trace map were to grow. Then when $x_k$ became large enough, the trace map would lead to exponential escape. This, however, is a contradiction, so we conclude that the traces at the Fibonacci points are bounded. As will be seen in the next section, in fact we expect that when suitably scaled, the $N$ transfer matrices $T(n)$ for a sample of $N$ sites are distributed with a stationary density. The Fibonacci points map onto the $\mathrm{Tr}T'=0$ surface, where $T'$ is the rescaled transfer matrix, and this stationary density does not vanish there, so the point is in the spectrum. This leads to the following conjecture.

*Conjecture II.* All points, for which the resistance as a function of sample size is bounded by a power of the sample length, are in the spectrum.

## V. EXAMPLES

In this section we illustrate the previous general results for the behavior of the resistance of a sample as a function of the sample length. As shown previously by Kohmoto *et al.*,[10] the Cantor set spectrum for these one-dimensional quasiperiodic systems is dominated at the center of the band by a 6-cycle of the trace map, and at the band edges by a 2-cycle of the trace map. Many analytic results are known for these cycles, not least of which are explicit formulas for their location. Thus in Sec. V A we study the 6-cycle, and in Sec. V B we study the 2-cycle. In Sec. V C we look at other cases.

The quantity we study is the natural logarithm of the square of the size of the transfer matrix $T(n)$, which we denote by $R(n)$. It in turn is related to the natural logarithm of the resistance $\rho(n)$ through

$$R(n)=\ln[|T(n)|^2]=\ln[2\rho(n)+1] \ge 0 .$$

### A. The six cycle

The choice $b=(0,1,0,0)$ and $a=(\cosh(\theta),0,\sinh(\theta),0)$ leads to a 6-cycle of the trace map. In fact, these matrices $B$ and $A$ also lead to a 6-cycle of the matrix map, so that no Lorentz transformation is needed to bring them into alignment. And finally, the matrices $B$ and $A$ generate an infinite but discrete subgroup of SL(2,$R$). Thus, the transfer matrices $T(n)$ sit on the discrete points of a lattice. In Fig. 1 we show $R(n)$ as a function of $n$, for $n$ from 1 to 400, and $\theta=1$. (We take $\theta=1$ for all subsequent examples of the 6-cycle.) The discrete structure is here clearly evident. We will always measure $R$ in units of $\ln(\phi)$, and the height of the picture frame in Fig. 1 is $36\ln(\phi)$.

We know by the previous arguments that $|T(n)|$ is bounded by a power of $n$, so in Fig. 2 we show $R(n)$ versus $\ln(n)$. The maximum $n$ in this picture is $N=F_{18}=4181$, so that the width of the horizontal frame is $\ln(F_{18})\approx 18\ln(\phi)$. The marks on the horizontal axis are at the Fibonacci numbers, so that they are spaced approximately by $\ln(\phi)$. The height of the vertical frame is $54\ln(\phi)$. In this picture, and henceforth, we will represent data values at the Fibonacci points by small boxes.

For very large $N$, the spacing between the discrete values of $R(n)/\ln(N)$ becomes small, while the maximum and minimum values approach constants. The minimum of course is zero, while the maximum is given by an exact calculation as $2/[3\ln(\phi)]=1.3854\ldots$ In Fig. 3 we show a histogram of the logarithm of the number of times $R(n)/\ln(N)$ takes the different discrete values. This again is the case where $N$, the maximum $n$, is $F_{18}=4181$. Sutherland[11,12] has calculated the limiting curve exactly, and this is shown in Fig. 4 for comparison. Thus, we can say that the resistance increases not by a single power of the distance, but instead has a spectrum of powers or exponents, given by the limiting distribution of Fig. 2. The analytic form is given in the paper of Sutherland.[12]

As we mentioned, the transfer matrices $T(n)$ for the 6-cycle are elements of a discrete group, and as shown by Kohmoto *et al.*,[10] can be represented in the form $T(n)=B^qA^r$, for $q=0,1,2,3$, and $r$ any integer. Figure 5 shows the distribution of the transfer matrices $T(n)$ themselves, and requires some explanation. First, the right-hand frame simply shows $R(n)$ versus $\ln(n)$; the units are as before. As we have emphasized, any transfer matrix $T(n)$ is specified by three parameters—say $a_0$, $a_1$, and $a_2$. In the left frame of Fig. 5, we project the transfer matrix $T(n)$ down onto the $a_0-a_1$ plane. There we use coordinates

$$x=[a_0/(a_0^2+a_1^2)^{1/2}]R(n)/\ln(N)\ ,$$

$$y=[a_1/(a_0^2+a_1^2)^{1/2}]R(n)/\ln(N)\ .$$

Thus the radius is $R(n)/\ln(N)$, which is the vertical quantity of the right frame. A visual inspection relates the scales in the two frames. The contour lines show the lines of constant trace with $a_0=-2$, $-1.5$, $-1$, $-0.5$, $0.5$, $1$, $1.5$, $2$. One finds the highly symmetrical structure corresponding to the discrete group, and an invariant distribution for the matrix.

### B. The two cycle

We now show a similar series of pictures for the 2-cycle, with $b=(3/4,7^{1/2},0,0)$ and $a=(3/2,3\times 7^{1/2}/17,77^{1/2}/14,0)$. In contrast to the 6-cycle, a Lorentz transformation is needed to bring the $A$ and $B$ matrices into alignment after two iterations. In Fig. 6, we show $R(n)$ versus $n$ for 400 sites. The units of this picture are the same as those of Fig. 1, so a direct comparison is possible. The contrast is striking.

Figure 7 is the counterpart for the 2-cycle of Fig. 2, where we show $R(n)$ as a function of $\ln(n)$. The values lie within a wedge of constant angular opening about a straight line with some average slope. This suggests we

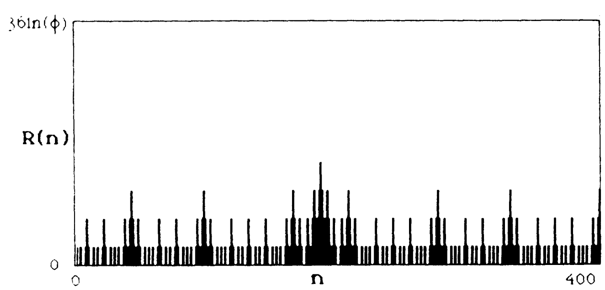


FIG. 1. The quantity $R(n)$ is shown as a function of $n$ for the 6-cycle.

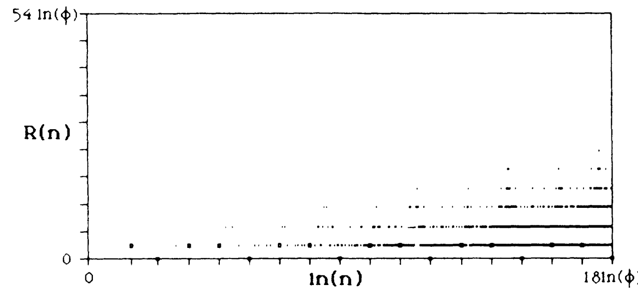


FIG. 2. The quantity $R(n)$ is shown as a function of $\ln(n)$ for the 6-cycle.

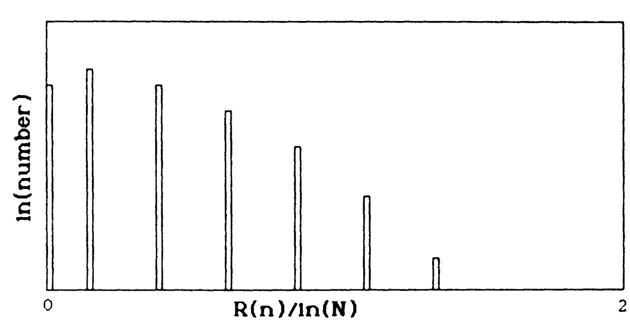


FIG. 3. A histogram of the logarithm of the number of sites with a given value of $R(n)/\ln(N)$ is shown, with $N=4181$ sites, for the 6-cycle.

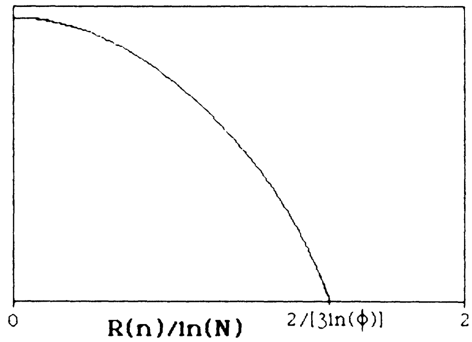


FIG. 4. Same as Fig. 3, showing the exact limiting curve for the 6-cycle.

examine the distribution of $R(n)/\ln(n)$, or equivalently of $R(n)/\ln(N)$, for scaling properties. Thus in Fig. 8 we show a histogram of the logarithm of the number of times $R(n)/\ln(n)$ takes various values. This once again is $N=F_{18}=4181$, but an increase in $N$ would give little change other than smoothing out the fluctuations of the histogram. [For the 2-cycle, we use a running rescaling by dividing $R(n)$ by $\ln(n)$, instead of $\ln(N)$ as was done for the 6-cycle, because the convergence is better. We then are not fighting the discrete structure of the 6-cycle.] The maximum value of the slope, equal to the upper edge of the histogram, is in excellent agreement with an exact calculation of Kohmoto *et al.*[10]

Finally, in Fig. 9 we show the distribution of the matrix itself in the $a_0$-$a_1$ plane. We now perform a running rescaling, so that the variables in the left frame are

$$x=[a_0/(a_0^2+a_1^2)^{1/2}]R(n)/\ln(n)\ ,$$

$$y=[a_1/(a_0^2+a_1^2)^{1/2}]R(n)/\ln(n)\ .$$

There is a surprising amount of structure in the scaling distribution of the matrix itself. In Figs. 10 and 11 we magnify the distribution $2\times$ and $4\times$, respectively, from Fig. 9. In contrast to this intricate structure, the distribution of the radii of the points, given in Fig. 8, we recall is smooth.

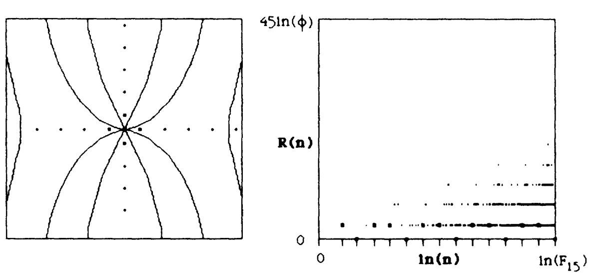


FIG. 5. The right frame shows $R(n)$ vs $\ln(n)$, while the left frame shows the distribution of the matrix, for the 6-cycle. The coordinates are explained in the text.

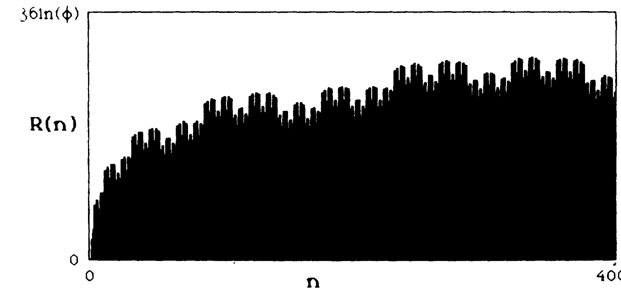


FIG. 6. The quantity $R(n)$ is shown as a function of $n$ for the 2-cycle.

### C. Other points

In contrast to the fixed points, we show in Fig. 12 a 10% deviation from the 6-cycle, where we take $b=(0,1,0,1,0)$ and $a=(\cosh(1),0,\sinh(1),0)$. This point is in the energy gap. The exponential increase of $R(n)$ and thus the resistance, accompanied by the escape of the matrix, is clearly evident.

## VI. CONCLUSION

We have shown that the resistance of the one-dimensional quasicrystals based on the Fibonacci scheme grows with sample size no faster than a power of the sample size. In fact, there is a distribution of different powers for the growth, leading to extremely large fluctuations of the resistance. It is conjectured that this behavior holds as well for all energies in the spectrum. It is interesting to compare the scaling behavior and fluctuations of this quasicrystal with that for random systems, as developed by Anderson *et al.*[13] and Lee and coworkers.[14]

## APPENDIX

Here we present all the mathematical details needed to prove the results used in Sec. IV to show the power-law increase of the resistivity. We break this appendix up into easily manageable sections. Many of these techniques were developed in another context by Sutherland.[15]

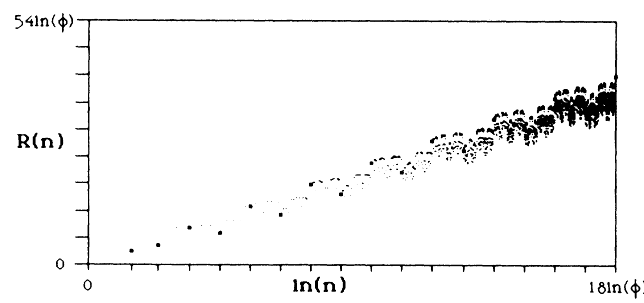


FIG. 7. The quantity $R(n)$ is shown as a function of $\ln(n)$ for the 2-cycle.

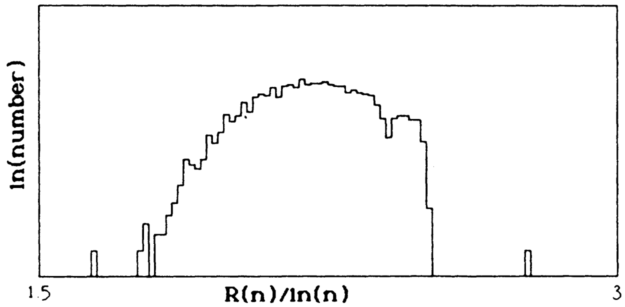


FIG. 8. A histogram of the logarithm of the number of sites with a given value of $R(n)/\ln(n)$ is shown, with $N=4181$ sites, for the 2-cycle.

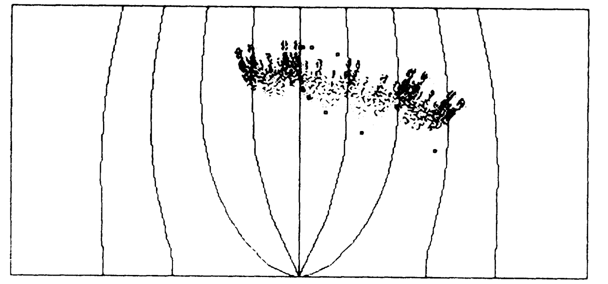

FIG. 10. This is a twofold enlargement of the left frame of Fig. 9.

### 1. Parametrization of the transfer matrices

The transfer matrices are elements of SL(2,$R$), the set of all real, $2\times2$ matrices with determinant one, and hence invertible. This is a subgroup of GL(2,$R$).

Let us introduce a basis for the $2\times2$ matrices as

$$\tau_0=1,\quad \tau_1=i\sigma_y,\quad \tau_2=\sigma_z,\quad \tau_3=\sigma_x\ ,$$

where $\sigma_j$ are the Pauli spin matrices. Thus the $\tau_j$ are real. Explicitly, they are given as

$$\tau_0=I=\begin{bmatrix}1 & 0\\ 0 & 1\end{bmatrix},\quad \tau_1=\begin{bmatrix}0 & 1\\ -1 & 0\end{bmatrix},$$

$$\tau_2=\begin{bmatrix}1 & 0\\ 0 & -1\end{bmatrix},\quad \tau_3=\begin{bmatrix}0 & 1\\ 1 & 0\end{bmatrix}.$$

We note

$$\mathrm{Tr}(\tau_0)/2=1\ ,$$

while

$$\mathrm{Tr}(\tau_j)/2=0,\quad j=1,2,3\ .$$

Also,

$$(\tau_0)^2=-(\tau_1)^2=(\tau_2)^2=(\tau_3)^2=I\ .$$

The multiplication rules are

$$\tau_1\tau_2=-\tau_3=-\tau_2\tau_1\ ,$$

$$\tau_2\tau_3=\tau_1=-\tau_3\tau_2\ ,$$

$$\tau_3\tau_1=\tau_2=-\tau_1\tau_3\ .$$

Then we can write a general matrix $A$ in SL(2,$R$) as

$$A=a_0\tau_0+a_1\tau_1+a_2\tau_2+a_3\tau_3 = \begin{bmatrix}a_0+a_2 & a_3+a_1\\ a_3-a_1 & a_0-a_2\end{bmatrix}.$$

The condition that the determinant is one translates into the following condition on the coefficients:

$$a_0a_0+a_1a_1-a_2a_2-a_3a_3=1\ .$$

This suggests that we parametrize the coefficients as

$$a_0=\cosh(\theta)\cos(\varphi),\quad a_1=\cosh(\theta)\sin(\varphi)\ ,$$

$$a_2=\sinh(\theta)\cos(\psi),\quad a_3=\sinh(\theta)\sin(\psi)\ .$$

The range of parameters can be chosen as either $-\pi<\varphi\le\pi$, $-\pi<\psi\le\pi$, $0\le\theta$, or $-\pi<\varphi\le\pi, 0\le\psi<\pi$.

The set of four coefficients $a_j$, subject to the constraint

$$1=a_0^2+a_1^2-a_2^2-a_3^2\ ,$$

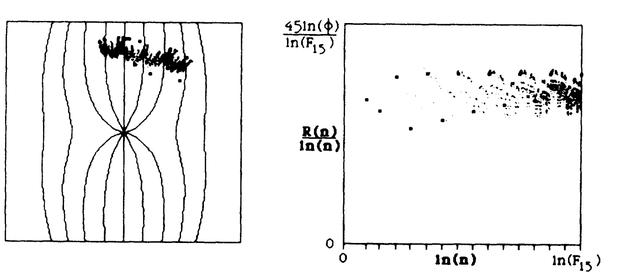


FIG. 9. The right frame shows $R(n)$ vs $\ln(n)$, while the left frame shows the distribution of the matrix, for the 2-cycle. The coordinates are explained in the text.

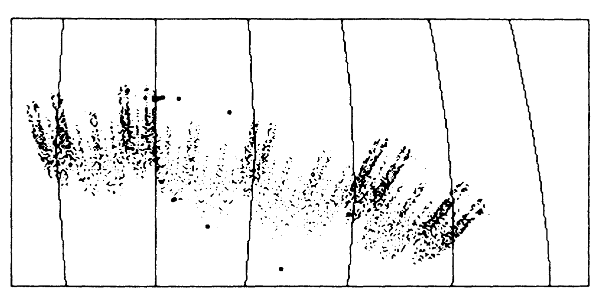

FIG. 11. This is a fourfold enlargement of the left frame of Fig. 9.

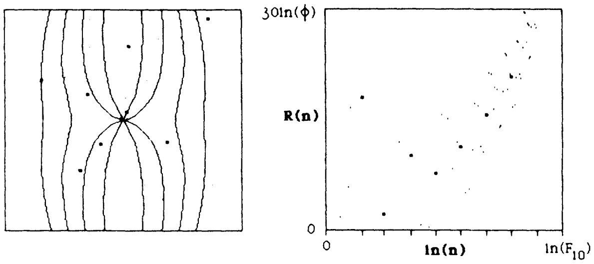


FIG. 12. The right frame shows $R(n)$ vs $\ln(n)$, while the left frame shows the distribution of the matrix, for a matrix which is not on a cycle. The coordinates are explained in the text.

will most often be used to parametrize the matrix $A$, and they will be represented collectively by the single symbol $a$. The parameters may also be viewed as components of a four-dimensional vector in Euclidean space. The constraint then defines a noncompact manifold, which we show in Fig. 13 by a cross section with $a_3=0$. In Fig. 14 we show the local coordinates about the identity matrix.

### 2. The invariant scalar product

The manifold of the group SL(2,$R$) is embedded in $E^4$, but the geometry of $E^4$ is not the natural geometry of the group. As we shall now show, instead there is an alternate scalar product, related to the constraint, which is invariant under the group action.

If $A$,$B$ are two matrices in SL(2,$R$), then when we multiply on the left-hand side by a third matrix in SL(2,$R$), we have

$$A,B \rightarrow A',B'=CA,CB \ .$$

Considering the form $(B,A)_G=\mathrm{Tr}(B^{-1}A)/2$ as a scalar product, we see that it is invariant under both left and right multiplication. The parameters $a_j$ are then obtained by projecting out on the $\tau$'s using this scalar product. In terms of the parameters, this scalar product becomes

$$(B,A)_G=b_0a_0+b_1a_1-b_2a_2-b_3a_3=(A,B)_G=(b,a)_G \ .$$

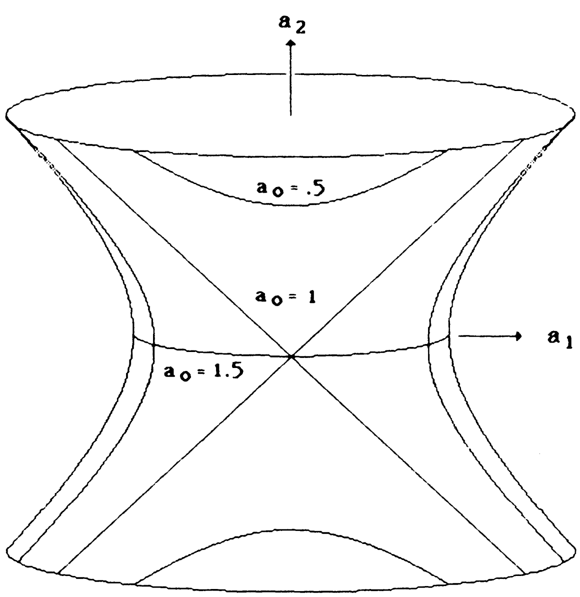


FIG. 13. A section of the parameter space of SL(2,$R$) with $a_3=0$, showing curves with $a_0$ constant. The $a_0$ axis comes out of the paper.

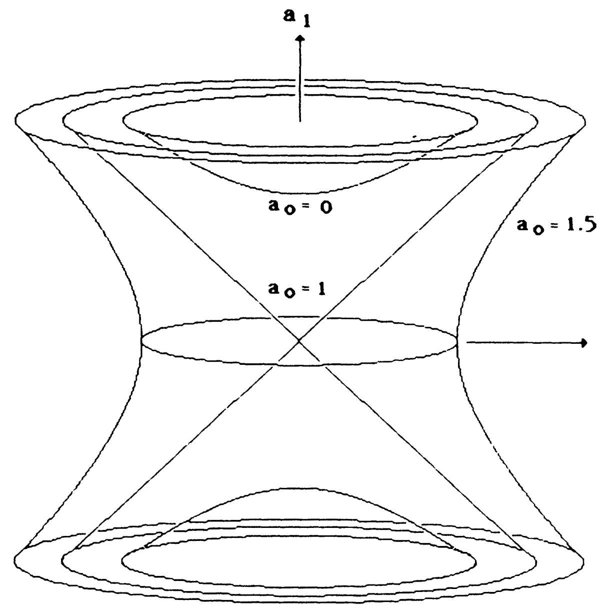


FIG. 14. The local coordinates about the identity element of SL(2,$R$). Surfaces of constant invariant distance from the identity are shown. The $a_2$ axis comes out of the paper.

### 3. Lorentz invariance

The group action, which is analogous to translations in that no point is left invariant, are not the only transformations which leave the scalar product invariant; nor is the group multiplication, and hence the Fibonacci dynamics, invariant under the group action. However, if we consider transformations of all elements $A$ in SL(2,$R$) by a single element $C$, through

$$A \rightarrow A'=CAC^{-1} \ ,$$

then we see that both

$$(A',B')_G=(A,B)_G \quad \text{and} \quad (AB)'=A'B' \ .$$

These are transformations which not only preserve the scalar product, but also leave invariant the identity element $I$. Thus, the scalar product of $I$ with any element $A$ is invariant under this transformation:

$$(I,A')_G=(I,A')_G=a_0 \ .$$

This implies that the scalar product

$$(B,A)_L=(B,A)_G-(B,I)_G(I,A)_G=b_1a_1-b_2a_2-b_3a_3$$

is invariant.

We thus call such a transformation

$$A\to A'=CAC^{-1}$$

a Lorentz transformation of $A$ by $C$. We write a general element $A$ with parameter $a$ as $A(a)$. Then for a Lorentz transformation $C$, we will have

$$A(a)\to A'=C(c)A(a)C^{-1}(c)=A(a')=A(L(c)a)\ ,$$

where $L(c)$ is the three-dimensional Lorentz transformation on the $a_1$-$a_2$-$a_3$ subspace, with parameter $c$. The mapping from $C(c)$ to $L(c)$ is two-to-one, since either choice $\pm C(c)$ leads to the same Lorentz transformation $L(c)$, much as the relation between SU(2) and the rotations O(3) is two-to-one. The Lorentz transformations include one-dimensional rotations about the $a_1$ axis, as well as boosts along a two-dimensional velocity vector in the $a_2$-$a_3$ plane. (One might like to consult Fig. 14 again to see the local geometry.)

#### 4. The set of Lorentz invariants

We have established that the scalar product $(A,B)_L$ is invariant under Lorentz transformations. For a single matrix $A$, $(A,A)_L$ is the only Lorentz invariant. However, for a pair of matrices $A,B$, the Lorentz invariants are $(A,A)_L$, $(B,B)_L$, $(A,B)_L$. Equivalently, we could take as the invariants $(I,A)_G=a_0$, $(I,B)_G=b_0$, $(A,B)_L$.

The traces of the matrices for the Fibonacci dynamics previously introduced in this paper have a simple relationship to these Lorentz invariants, for

$$\mathrm{Tr}(A)/2=a_0,\quad \mathrm{Tr}(B)/2=b_0\ ,$$

while

$$\mathrm{Tr}(BA)/2=a_0b_0-a_1b_1+a_2b_2+a_3b_3$$
$$=a_0b_0-(b,a)_L\ .$$

Furthermore, these three invariants are a complete set of invariants for the ordered matrix pair $(B,A)$. Thus, if we have another matrix pair, $(B',A')$ with the same invariants, then there exists a unique Lorentz transformation $L$ which will bring the two pairs into alignment:

$$(B',A')=L(B,A)L^{-1}\ .$$

We make use of this observation in the following way.

Suppose we find a $Q$-cycle of the trace map. Since the traces of three consecutive matrices repeat, this means that the Lorentz invariants of two consecutive matrices, say $B_{k+Q}=T_{k+Q-1}$ and $A_{k+Q}=T_{k+Q}$, repeat as well. Thus the $Q$-times iterated pair $(B_{k+Q},A_{k+Q})$ is equivalent by a Lorentz transformation to the original pair $(B_k,A_k)$, or

$$(B_{k+Q},A_{k+Q})=L(B_k,A_k)L^{-1}\ .$$

Since the matrix dynamics is invariant under Lorentz transformations, we emphasize that the Lorentz transformation is the same for all $k$.

Therefore, an invariant set of the matrix map corresponding to the $Q$-cycle of the trace map is the set of all distinct pairs of matrices $L^n(B_k,A_k)L^{-n}$, for all integers $n$, and $k=1$ to $Q$. These sets lie within the $Q$ one-parameter submanifolds $L^n(B_k,A_k)L^{-n}$, where the parameter $n$ is now any real number. More-complicated invariant sets of the trace map than $Q$-cycles can likewise be treated.

#### 5. Determining the Lorentz transformation

We now show how the Lorentz transformation is determined. Suppose we have a matrix pair $(B,A)$. Apart from an arbitrary Lorentz frame, they are specified by the set of three Lorentz invariants, which we take to be $\{\mathrm{Tr}(B)/2,\mathrm{Tr}(A)/2,\mathrm{Tr}(BA)/2\}$ and denote collectively as $\mathbf{r}$. We choose our Lorentz frame to bring the matrix pair into a standard alignment, which we take as

$$A=a_0\tau_0+a_1\tau_1\ \text{ if } A \text{ is timelike}\ ,$$

$$A=a_0\tau_0+a_2\tau_2\ \text{ if } A \text{ is spacelike}\ ,$$

$$B=b_0\tau_0+b_1\tau_1+b_2\tau_2,\quad b_1,b_2>0\ .$$

We write this initial pair, in standard alignment, with parameter $\mathbf{r}$ as $(B[\mathbf{r}],A[\mathbf{r}])$.

We now iterate the matrix map once to give the new matrix pair $(B',A')=(A,BA)$ with parameter $\mathbf{r}'$, which is the old parameter $\mathbf{r}$ iterated once by the trace map. This new matrix pair is not in standard alignment. It can, however, be brought into standard alignment by a Lorentz transformation $S$, to that

$$(B',A')=S[\mathbf{r}](B[\mathbf{r}'],A[\mathbf{r}'])S[\mathbf{r}]^{-1}\ .$$

The notation is as follows: A pair $(B[\mathbf{r}],A[\mathbf{r}])$ will always denote a matrix pair, in standard alignment, with parameter $\mathbf{r}'$. We start with a pair $(B[\mathbf{r}],A[\mathbf{r}])$ in standard alignment, so that after iteration, the pair $(B',A')$ is completely determined by the parameter $\mathbf{r}$; in particular, the parameter $\mathbf{r}'$ is determined by $\mathbf{r}$ through the trace map. However, the orientation of the pair $(B',A')$ is also determined uniquely by $\mathbf{r}$, so the Lorentz transformation $S$ needed to bring the pair $(B',A')$ into the standard alignment $(B[\mathbf{r}'[,A[\mathbf{r}'])$ is uniquely determined by $\mathbf{r}$. We write this dependence of $S$ on $\mathbf{r}$ as $S[\mathbf{r}]$. It is *not* a Lorentz transformation $S(r)$ with parameter $r$; that is why we denote it by the symbol $S[\mathbf{r}]$ instead of $S(r)$.

Now, by repeating this procedure each time, as we iterate the matrix map $k$ times, we obtain

$$(T_{k+1},T_k)=S[\mathbf{r}_1]\cdots S[\mathbf{r}_k](B[\mathbf{r}_{k+1}],A[\mathbf{r}_{k+1}])S[\mathbf{r}_k]^{-1}\cdots S[\mathbf{r}_1]^{-1}\ .$$

The orbit of the trace map is $(\ldots,\mathbf{r}_k,\mathbf{r}_{k-1},\ldots,\mathbf{r}_2,\mathbf{r}_1)$. Thus if we have a $Q$-cycle of the trace map, so that $\mathbf{r}_{Q+1}=\mathbf{r}_1$, then we can make the identification

$$L=S[\mathbf{r}_1]\cdots S[\mathbf{r}_Q]\ .$$

This expression must be invariant if we translate along the orbit of the trace map.

### 6. The Euclidean metric

Although the scalar product

$$a_0b_0+a_1b_1-a_2b_2-a_3b_3 =(a,b)_G=(A,B)_G=\mathrm{Tr}(A^{-1}B)/2$$

is very natural and useful, since it is invariant under the group action, and the Lorentz metric

$$a_1b_1-a_2b_2-a_3b_3 =(a,b)_L=(A,B)_L=(A,B)_G-(A,I)_G(I,B)_G$$

is even more useful, since it is invariant under the Lorentz transformations, which are a symmetry of the Fibonacci dynamics, neither of these are useful for estimating the size of a matrix. For instance, $(A,A)_G=1$, while $(A,A)_L$ is not positive definite. On the other hand, if we try to use $[(A,I)_G]^2=a_0^2=[\mathrm{Tr}(A)/2]^2$ as an estimate of a size of a matrix, we find that we can multiply two matrices, each of which have zero trace, to get a product which has a trace arbitrarily large. As such an example, take $A=[1+a^2]^{1/2}\tau_1+a\tau_2$. Then $\mathrm{Tr}(A)/2=0$ and $\mathrm{Tr}({}^tA)/2=0$, while $\mathrm{Tr}({}^tAA)/2=1+2a^2$.

Clearly, what is needed for estimating the size of a matrix is a Euclidean scalar product, which is positive definite, and has the triangle inequality for estimating the size of a product from the sizes of the factors. However, as we have seen, such a scalar product cannot be invariant under the same Lorentz symmetry as the Fibonacci dynamics.

The manifold $(A,A)_G=1=(a,a)_G$ is embedded in the fourth-dimensional Euclidean space, and this provides us with the scalar product

$$a_0b_0+a_1b_1+a_2b_2+a_3b_3 =(a,b)=(A,B)=\mathrm{Tr}({}^tAB)/2=(B,A)\ .$$

This gives us our definition for the size $|A|$ of the matrix $A$ as

$$|A|^2=(A,A)=\mathrm{Tr}({}^tAA)/2=a_0^2+a_1^2+a_2^2+a_3^2 =(a,a)={}^taa\ .$$

We easily establish that for $A$ in SL(2,$R$)

$$|A|^2=1+2(a_2^2+a_3^2)=\cosh(2\theta)\geq 1\ ,$$

$$|A|=|A^{-1}|=|{}^tA|\ ,$$

and

$$|A|\geq(I,A)=(I,A)_G=a_0\geq -|A|\ .$$

### 7. Growth of a product

We now wish to establish the important result that given $A,C$ in SL(2,$R$),

$$|AC|^2\leq 2|A|^2|C|^2\ .$$

First, let $B=AC$. Then, we can write right multiplication by $C$ as $b=R(C)a$, where $R(C)$ is a $4\times4$ matrix representation. Now,

$$|B|^2={}^tbb={}^ta\,{}^tR(C)R(C)a\geq{}^taa\Lambda^2=\Lambda^2|A|^2\ ,$$

where $\Lambda^2$ is the maximum eigenvalue of the symmetric, positive definite matrix ${}^tR(C)R(C)$.

By orthogonal rotations of the form $\mathrm{O}(1)\times\mathrm{O}(1)$ on the $a_0$-$a_1$ and $a_2$-$a_3$ subspaces, which will not change the eigenvalues of ${}^tR(C)R(C)$, we can put $C$ in the standard form

$$C=\exp(\theta\tau_2)\ ,$$

a pure "boost." Then $R(C)$ is easily evaluated as

$$R(C)=\begin{bmatrix}\cosh(\theta) & 0 & \sinh(\theta) & 0\\ 0 & \cosh(\theta) & 0 & -\sinh(\theta)\\ \sinh(\theta) & 0 & \cosh(\theta) & 0\\ 0 & -\sinh(\theta) & 0 & \cosh(\theta)\end{bmatrix}$$

and

$${}^tR(C)R(C)=\begin{bmatrix}\cosh(2\theta) & 0 & \sinh(2\theta) & 0\\ 0 & \cosh(2\theta) & 0 & \sinh(2\theta)\\ \sinh(2\theta) & 0 & \cosh(2\theta) & 0\\ 0 & \sinh(2\theta) & 0 & \cosh(2\theta)\end{bmatrix}.$$

The eigenvalues are clearly doubly degenerate, and equal to $\exp(\pm2\theta)$. Thus

$$\Lambda^2=\exp(2\theta)\leq 2\cosh(2\theta)=2|C|^2\ .$$

This establishes the result.

We note that if we take $C=A$, then the inequality gives

$$|A^2|^2=\cosh(4\theta)=2\cosh^2(2\theta)-1 \leq 2|A|^4=2\cosh^2(2\theta)\ ,$$

which approaches an identity for large $|A|$.

As a corollary, we also have

$$|CAC^{-1}|\leq 2|A|\,|C|^2\ .$$

[1]M. Kohmoto, L. P. Kadanoff, and C. Tang, Phys. Rev. Lett. **50**, 1870 (1983).
[2]S. Ostlund, R. Pandit, D. Rand, H. J. Schellnhuber, and E. Siggia, Phys. Rev. Lett. **50**, 1873 (1983).
[3]B. Simon, Adv. Appl. Math. **3**, 463 (1982); J. B. Sokoloff, Phys. Rep. **126**, 189 (1985).
[4]M. Kohmoto, Phys. Rev. Lett. **51**, 1198 (1983); S. Ostlund and R. Pandit, Phys. Rev. B **29**, 1394 (1984).
[5]R. Landauer, Philos. Mag. **21**, 683 (1970).
[6]M. Kohmoto, Phys. Rev. B **34**, 5043 (1986).
[7]M. Kohmoto and Y. Oono, Phys. Lett. **102A**, 145 (1984).
[8]A. Suto (unpublished).
[9]M. Kohmoto and J. R. Banavar, Phys. Rev. B **34**, 563 (1986).
[10]M. Kohmoto, B. Sutherland, and C. Tang, Phys. Rev. B **35**, 1020 (1987).
[11]B. Sutherland, Phys. Rev. B **34**, 3904 (1986).
[12]B. Sutherland, Phys. Rev. B **35**, 9529 (1987).
[13]P. W. Anderson, D. J. Thouless, E. Abrahams, and D. S. Fisher, Phys. Rev. B **22**, 3519 (1980).
[14]P. A. Lee and A. D. Stone, Phys. Rev. Lett. **55**, 1622 (1985); H. Fukuyama, P. A. Lee, and A. D. Stone (unpublished).
[15]B. Sutherland, Phys. Rev. Lett. **57**, 770 (1986).